EasyChair Preprint

№ 15404

Measurement and Modelling of Friction for Cylindrical Gears with Pitch Line Velocities up to 100 M/S

Mathis Steinrötter, Jaacob Vorgerd, Alexander Thomas and Manuel Oehler

November 10, 2024

Measurement and modelling of friction for cylindrical gears with pitch line velocities up to 100 m/s

1st Mathis Steinrötter
Ruhr University Bochum
Chair of Drive Technology
Bochum Germany
mathis.steinroetter@rub.de

2nd Dr. Ing Jaacob Vorgerd
Ruhr University Bochum
Chair of Drive Technology
Bochum Germany
jaacob.vorgerd@rub.de

3rd Alexander Thomas
Ruhr University Bochum
Chair of Drive Technology
Bochum Germany
alexander.thomas-z4j@rub.de

4rth Prof. Dr. Ing Manuel Oehler
Ruhr University Bochum
Chair of Drive Technology
Bochum Germany
manuel.oehler@rub.de

***Abstract*— Current political efforts to meet global climate goals require efficient propulsion systems for industrial and mobile applications. Optimizing efficiency also offers significant potential for energy cost savings. Reducing friction through tribologically optimized contacts helps minimize power losses and maximize load capacity. Gear friction is a transient phenomenon since tribological conditions change over the path of contact. Various models exist for calculating gear friction, but they show significant differences under the same conditions, particularly in the high-speed regime where experiments are lacking. To close this gap experiments were conducted to measure gear power losses using calorimetric properties in a high-speed back-to-back gear test rig. Factors such as pitch line velocity, surface topography, lubricant temperature and gear geometry were studied. Based on experiments, an existing friction model was calibrated adjusting parameters like topography, load, and speed. The pitch line velocity significantly influenced gear friction, with higher velocities reducing friction due to hydrodynamic effects. Test specimens with isotropic superfinishing showed a mean friction coefficient about 30 % lower than ground gears. The adjusted friction model helps evaluate load dependent power losses, improving efficiency in mobility and aviation, contributing to more sustainable transportation.**

Keywords—gear friction, high speed efficiency, superfinishing

I. Introduction

Current political initiatives aimed for achieving global climate goals highlight the urgent need for more efficient drive trains. Enhancing efficiency not only addresses environmental concerns but also offers significant opportunities for cutting operational costs. The reduction of power losses in drive trains has become increasingly important, particularly as electric vehicles continue to gain popularity in the private mobility sector. The limited electric range of these vehicles remains a significant barrier to their widespread adoption for everyday use, and this range is directly impacted by power losses within the drive train. By reducing friction in gear transmissions, it is possible to increase the vehicle's driving range without requiring additional battery capacity. Beyond road mobility, the efficiency of drive trains is also crucial in civil aviation, where both high energy costs and the need to reduce climate-sensitive emissions are pressing concerns. Furthermore, in aviation, the high temperature and mechanical stress in jet turbines present additional challenges, as they can limit the overall performance of drive trains in this sector.

To achieve this, it is essential to optimize the geometry and tribological properties of gears to increase their load-carrying capacity. Reducing friction in slide-to-roll contacts, particularly through tribological optimization, helps minimize power losses and improve load-carrying performance [1]. Therefore, incorporating low-friction gears is a key strategy for advancing more sustainable drive technologies. One action for optimizing gearbox efficiency is the use of isotropic superfinished gears. This process results in a surface topography that significantly enhances frictional properties [2, 3]. Improvements in friction reduction have been demonstrated in standardized tests, as well as in analogous experiments using a 2-disc tribometer [4].

II. State of the Art

A. Gear Power losses

The efficiency of gearboxes is influenced by several parameters. Different machine elements are part of power losses, which reduce the gear box efficiency [5]. Gears, bearings and sealings are the main power loss influences. In this paper the gear power losses are examined in detail. These are divided in load dependent and load independent losses. Load dependent power losses P_{VZP} are the integral of the locally dissipated frictional power ($\mu \cdot F_N \cdot v_g$) in each roll angle. The meshing of gears can alternatively be described by the engagement time t_E to take account for influences of elasticity on the line of action. Addressing gear geometry, the length and position of the line of action affect the formation of load dependent power loss. This is done by addressing these influencing factors in the power loss factor H_{VL} (2) [6–8]. The load dependent power losses are calculated with the driving power, which is transmitted with the gear contacts multiplied with a mean coefficient of friction μ_m and the influence factor H_{VL}, (1). This factor is evaluated by the product of the normalized normal force and the normalized sliding velocity integrated over the tooth width and the contact time. The aim of this is to get the influences of the load distribution and flank modifications on the power losses. With higher loads the line of action of gear flanks gets longer and gear mesh areas with high sliding velocities are in contact. This phenomenon leads to increasing power losses.

$$P_{VZP} = P_a \cdot \mu_m \cdot H_{vL} \tag{1}$$

$$H_{VL} = \frac{1}{t_E} \int_0^{t_E} \int_0^{l_{eff}} \frac{f_N(t,y)}{F_{tb}} \cdot \frac{v_g(t,y)}{v_{tb}} \, dy \, dt \tag{2}$$

In addition to the load dependent shares, the absolute gear power loss P_{VZ} is influenced by a load independent component, (3). The load independent power loss P_{VZ0} results from fluid mechanical effects of the rotating gears in an air-oil environment. The primary influence factors are the pitch line velocity v_t and rheological properties of the lubricant. Furthermore, the load independent power loss is affected by the mechanical design of the gearbox components and the explicit design of the lubrication system [9, 10].

$$P_{VZ} = P_{VZP} + P_{VZ0} \tag{3}$$

B. Gear friction

In current practice, several models are available for calculating gear friction [11–17]. However, these models often yield significantly different results, even under identical operating conditions. Most of these models are calibrated using experimental data from conventionally ground gears, and their accuracy when applied to alternative surface topographies is not always guaranteed. Since topography cannot be fully represented by roughness parameters alone, it is typically accounted for using empirical influence factors [11, 15, 18, 19].

Isotropic superfinished gears are not yet widely covered in these models. Therefore, the analysis in Fig. 1 incorporates isotropic superfinishing by considering the reduction in profile roughness to $Ra = 0.1\,\mu m$. A comparison of gear friction models reveals a significant variation in results, although all models show a general trend of reduced friction coefficients due to isotropic superfinishing. However, the degree to which they weight this effect varies across the models.

C. Isotropic Superfinishing

In conventional gear manufacturing, the gear geometry is created in hard machining after the heat treatment process [20]. The surface texture, along with the interaction between the lubricant, material, and load, significantly affects frictional performance [21, 22]. The purpose of isotropic superfinishing is to refine the surface by carefully removing the outer layer without introducing additional thermomechanical stress, thereby maintaining the existing residual stress profile. This process involves the use of micrometer-sized ceramic particles in a labor-intensive grinding procedure. As a result a surface with an isotropic texture and a profile roughness (Ra) of less than 0.1 µm [4, 23, 24] can be created. The surface treatment removes surface peaks while retaining the valleys formed during the hard machining phase [25]. Tests on stationary disc contacts [1] have shown that isotropic superfinished surfaces can reduce friction by as much as 30 % compared to conventionally ground surfaces. Studies by SOSA [4] further confirmed these friction-reducing benefits in gear applications.

D. Discussion

There are several different models to calculate the coefficient of friction in the gear mesh. Fig. 1 shows a comparison of five different approaches [13–17]. In this simulation the mean coefficient of friction for a FZG-C type gear at load point of $T_1 = 200$ Nm and $v_t = 80$ m/s is shown. On the one hand this comparison expresses the significant difference in the friction coefficients between each other. On the other hand, it shows the influence of the arithmetic mean roughness Ra in every calculation approach. A reduction of the Ra value from $Ra = 0.5$ µm to $Ra = 0.1$ µm leads to a 10-35 % lower coefficient of friction depending on the used model.

In general, most of these approaches do not address the local slide-to-toll ratio in the calculation. Studies from LÖPENHAUS [15] clarify the dependency of this in evaluating the mean coefficient of friction μ_m. None of these models were calibrated with experimental data for the high-speed range up to pitch line velocities of $v_t = 100$ m/s. The application of the approaches shown in [13–17] for this range is questionable.

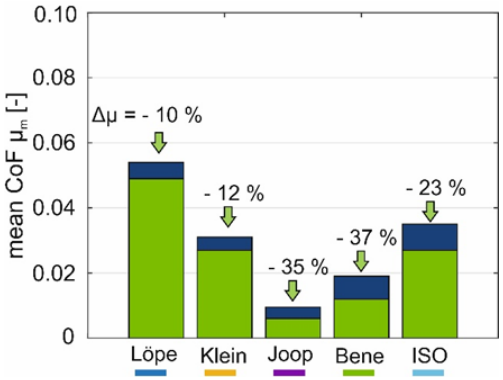

Fig. 1. Comparison of mean CoF for FZG-C-type gear at v_t = 50 m/s and T_2 = 200 Nm with different friction models for ground (blue) and superfinished (green) gears

III. METHOD

A. Load distribution and loaded gear mesh

The calculation of local loads in the gear mesh is carried out according to the method by WALKOWIAK [26]. In this model, the gear mesh is discretized and for each calculation point, the internal loads, local velocities, and EHL (elasto-hydrodynamic lubrication) parameters are determined. Each contact point in the gear mesh between initial contact and disengagement is described by the calculation. The quasi-static tangential force at the base circle is divided among the teeth engaged in the present contact situation in all discrete mesh positions. The elastic tooth contact is modeled based on the introduced load. The load distribution is calculated using the tooth and mating stiffnesses through the method of displacement influence numbers. In the displacement influence number $\overline{(a_k)}$ (4), both the deformations of the wheel body, HERTZIAN deformation, and tooth deflection are taken into account (7).

$$\sum_{j=1}^{n_b} \overline{a_k} \cdot \overline{F_{n,k,j}} = \overline{\delta_z - \delta_{k,j}} \tag{4}$$

$$\sum_{k=1}^{z_E} \sum_{j=1}^{n_b} r_{k,j} \cdot F_{n,k,j} = T_{ges} \tag{5}$$

The local velocities can be calculated from the trajectory of the contact points. These are particularly important for gear friction and the calculation of the lubricant film thickness.

Especially, the sliding and entrainment velocities are of interest. The velocity normal to the flank must be identical for both flanks due to the normal engagement at the contact point. The entrainment velocity (6) represents the sum of the tangential velocities present at the contact point. It matters in the subsequent calculation of the EHL conditions. In contrast, the sliding velocity (7) indicates the extent to which the contact partners slide over each other. Accordingly, it is calculated from the difference of the local tangential velocities.

$$v_\Sigma = v_{t1} + v_{t2} \tag{6}$$

$$v_g = v_{t1} - v_{t2} \tag{7}$$

B. *Measurement of power losses*

In the state of the art, the local gear friction cannot be measured directly. The local coefficient of friction is calculated using the mean CoF from the gear mesh. As seen in (1) the load dependent gear power loss depends on the mean CoF. To measure gear power losses a calorimetric measurement via the lubricant temperature is used. The physical principle behind this process assumes that all power loss is dissipated as heat. Under steady-state thermal conditions, the heat absorbed by the lubricant $\dot{Q}_{oil}$ is equivalent to the gear's power loss P_{VZ}. The amount of heat absorbed by the lubricating oil can be determined by measuring the inlet and outlet temperatures θ_{in} and θ_{out}, as well as the volumetric flow rate $\dot{V}_{oil}$. Additionally, the specific heat capacity c_p and density ρ_{oil} of the lubricant are taken into account, as shown in (8).

$$\dot{Q}_{oil} = c_p \cdot \rho_{oil} \cdot \dot{V}_{oil} \cdot (\theta_{out} - \theta_{in}) = P_{VZ} \tag{8}$$

To insulate the gear power losses from other sources of dissipated heat, such as bearings and seals, the test gears are enclosed in a specially designed insulated housing (see Fig. 2). The gear lubrication is separated from the bearing lubrication which allows the control over volumetric flow, injection pressure, and oil temperature independently. The insulation housing is made from temperature-resistant PEEK polymer. Both shafts are supported by the steel housing and are led out of the insulated enclosure through small gaps, which prevent contact between the shafts and housing plates. Because the gearbox uses contactless seals, the only significant source of thermal error comes from the bearings. The insulation housing effectively prevents convective heat exchange between heat sources, ensuring that heat transfer between the bearings and test gears occurs only through conductive connections via the common shafts. A thermal simulation of the setup showed that the conductive heat transfer through the shafts accounts for approximately 5-8% of the total heat under high-speed conditions [3].

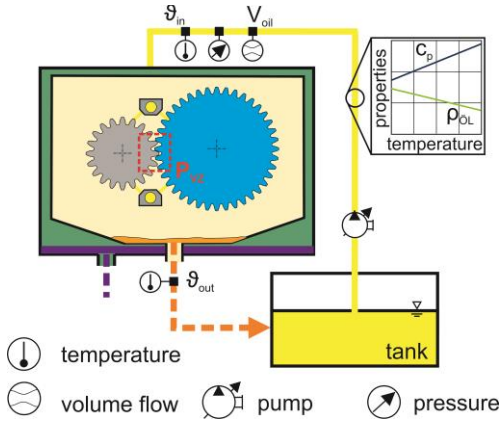

Fig. 2. Measurement of gear fritcion with oil inlet and outlet temperatures

C. *Test specimens*

The efficiency measurements were performed using two different variants of test gears, as outlined in TABLE I. To reduce gear dynamics at high pitch line velocities, both variants featured a deep tooth profile with a normal overlap ratio of $\epsilon_\alpha = 2$. Additionally, both gear variants were profile-modified to mitigate the effects of elasticity and avoid premature contact. For variant Geom B, a positive profile shift was incorporated to focus the main load events in the recess contact. The tip relief on the test gears in profile direction has an influence on the load sharing in the loaded gear mesh. This influence is shown in the H_{VL} factor for the gear geometry under its load conditions in the evaluated operating point. The aim in the efficiency reduction is to reduce the H_{VL} factor to achieve lower power losses in the gear mesh. The tip relief reduces the HERTZIAN pressure in gear mesh positions with high sliding velocities. During the experimental investigations, a synthetic ester-based oil of MIL-PRF-23699 specification was used.

TABLE I. GEOMETRY DATA TEST GEARS

Denomination	**Gear geometry data**			
	Symbol	***Unit***	***Geom A***	***Geom B***
Normale modulus	m_n	mm	4.825	5.625
Number of teeth	z_1 / z_2	-	35 / 39	30 / 42
Active tooth width	b_1 / b_2	mm	22 / 20	16 / 14
Normale pressure angle	α_n	°	22.5	20.0
Helix angle	β	°	5	5
Profile shift	x_1 /x_2	-	0.2000 / -0.2195	0.3000 / -0.2899
Overlap	ε_α	-	2.00	2.00
Active tip circle	d_{a1}/ d_{a2}	mm	183.93 / 247.69	187.04 / 248.17

The test specimens were manufactured through conventional hard-fine machining, specifically using the profile grinding process after case hardening. This process resulted in a profile roughness of $Ra = 0.32\,\mu m$, characterized by a symmetrical distribution of valleys and peaks in the Abbott curve, typical for profile-ground gears in industrial gearboxes [24]. Following this, isotropic superfinishing was applied. Fig. 3 compares the surface topographies of a ground and a superfinished flank. The chemical superfinishing leads to a significant reduction in

profile height. The final gear flanks achieved a profile roughness of $Ra < 0.10\ \mu m$. The ground surface shows the typical grinding grooves in lead direction. These are removed in the superfinishing process resulting in an isotropic surface texture.

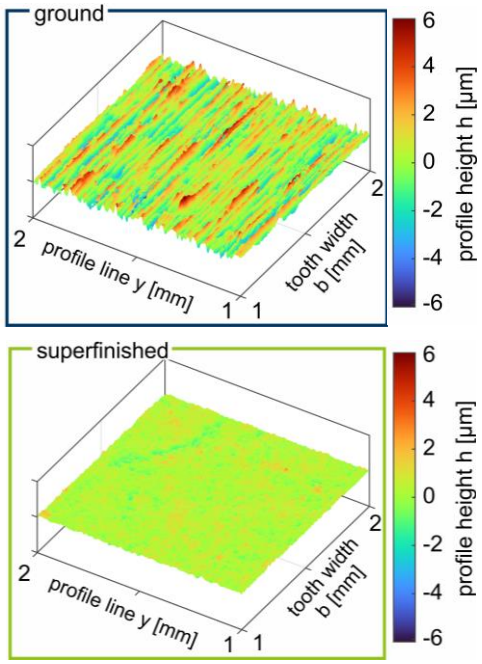

Fig. 3. Surface topography of ground and superfinished gear flanks from the test gears

D. Test procedure

In the experimental efficiency tests there are several parameters varied. The tests are carried out using the two gear geometries mentioned in Section III.C. The pitch line velocity v_t varies from 20 to 95 m/s in 5 speed levels. The load torque is set in six different load levels. Also, the tests are carried out both with a ground and isotropic superfinished surfaces. Furthermore, the inlet temperature of the lubricant was varied between $\theta_{in} = 80 \ldots 120$ °C. At a constant pitch line velocity, the load torque is progressively increased across several load stages. The methodology for assessing gear power losses is illustrated in Fig. 4 The runtime for each load stage is determined by the time it takes for the gearbox to reach a steady-state temperature. The adjustment of load levels is automated, allowing transitions between stages without shutting down the test rig.

E. Evaluating CoF

Based on the experimental test points with different speed and torque levels the mean coefficient of friction is evaluated from the recorded data. As explained in section III.B, the dissipated heat from the tooth contact is recorded. Using the temperature difference between the oil inlet and outlet of the gearbox, the power loss from the gear contact is calculated according to (8). This calculation includes both the load-independent and load dependent components of power loss. As the load stages increase, the absolute power loss also rises. To distinguish between the load dependent and load-independent components, the data points are subjected to linear regression. The load-independent power loss is represented by the intercept on the ordinate, while the difference between the total power loss and the load independent value represents the load dependent power loss. With the calculation of the load independent power loss shares the load dependent power losses can be evaluated. By using the calculated P_{VZP} and geometry factor H_{VL} for the corresponding gear geometry the mean friction coefficient in the selected test point can be evaluated by transforming (1) to μ_m. This procedure is used for every test point in the experimental test program.

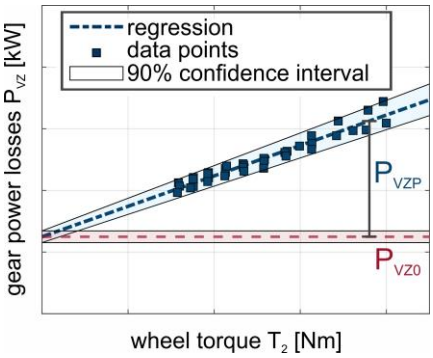

Fig. 4. Evaluation of load dependent and independent gear power losses from the total gear power losses

IV. Results

The following section shows the results of the experimental tests. Based on the tests carried out the mean coefficient of friction for each test point is evaluated. With this database and the friction model approach from Löpenhaus [15], a modified calculation model is presented. This allows to calculate the coefficient of friction for every contact situation in the gear mesh.

A. Power loss geometry factor

The power loss geometry factor, explained in section II.A does account the influence of the local loads and velocities in the elastic gear mesh on the power losses. The calculation of the load distribution is essential for this evaluation. The changes in the load distribution, especially when the gears do have a tip relief, influences the length and position of the line of action. The H_{VL} factor is essential for the evaluation of the mean coefficient of friction,

Fig. 5 shows a simulative comparison of the H_{VL} factor for the two gear geometries, Geom A and Geom B, which were used in the experimental tests. By increasing the load torque first, the power loss factor increases linear. With higher torques the gradient of both curves flattens. In the case of Geom A the drop of the gradient starts at lower torque levels at around $T_2 \approx 1000$ Nm compared to $T_2 \approx 1500$ Nm for Geom B. These gear geometries differ especially in the normal module, the normal pressure angle and the amount of the tip relief applied. Geom B has a larger tip relief and is specifically higher loaded, which leads to a generally higher power loss factor. The differences in the drop of the gradient lies within the higher amount of the tip relief of Geom B. By increasing the load torque, the line of action gets longer, because the profile modified parts of the gear

flank get into contact. These gear mesh positions are exposed to high sliding velocities. The H_{VL} factor is influenced by the multiplications of the normalized normal contact force and the normalized sliding velocity in the gear mesh positions. With the elastic deformation of the tooth and the longer line of action the power losses rise. When the tip relief is exceeded due to the tooth bending the gradient of the of the H_{VL} factor flattens.

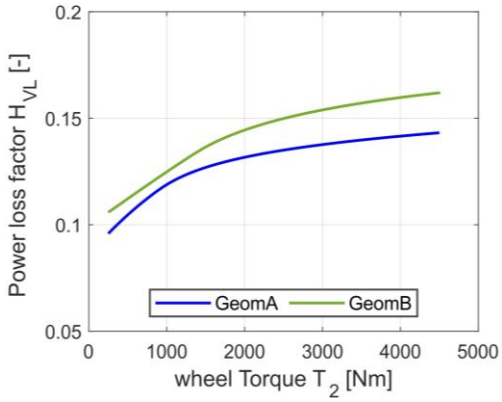

Fig. 5. Caluclated power loss factor H_{vL} for the two test gear geometries (Geom A and Geom B) over the load wheel torque

B. Influence of parameters on the coefficient of friction

In the experimental tests there were two different gear flank topographies tested. In the first test series the flanks were conventional hard machined and had a ground surface. The second test series included superfinished flanks (see Section III.C). The speed range for the test points was between $v_t = 20 - 95$ m/s. Fig. 6 shows the mean coefficient of friction over the pitch line velocity for both surface topographies. The coefficient of friction is evaluated from the load dependent power losses in the gear mesh with the consideration of the H_{VL} factor, as explained in Section II.A. By increasing the pitch line velocity v_t the coefficient of friction is reduced degressively. In the tests using ground gears, it decreases by about 28 % in the tested speed range. This reduction can be observed qualitatively for both topographies. Under the same boundary conditions (load, speed) friction coefficients are measured with smoother surfaces (isotropic superfinish), which are 30 % smaller than in the tests with profile ground gears without isotropic superfinishing.

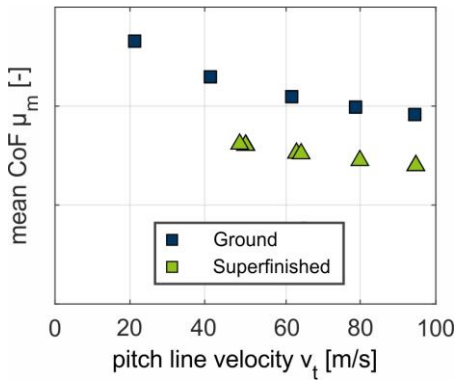

Fig. 6. Mean CoF over the pitch line velocity v_t for ground and Superfinished gears of gear geometry Geom B

In the tests different parameters were varied. As shown in Fig. 6 the pitch line velocity range is $v_t = 20 - 95$ m/s. Apart from the different surface topographies the two gear geometries Geom A and Geom B are used. Three different oil inlet temperatures from $\theta_{oil} = 80 \ldots 120\ °C$ are tested. The tests are carried out at different torque levels. Fig. 7 shows three comparisons of the coefficient of friction with different variations. The left two bars compare the CoF using Geom A and Geom B at the same load torque ($T_2 = 1900$ Nm) and the same oil inlet temperature ($\theta_{oil} = 100\ °C$). The differences between these friction coefficients are small with about 2% reduction for Geom B. For the variation of the torque the CoF also shows comparable values for both presented levels. By increasing the torque from $T_2 = 1900$ Nm to $T_2 = 4000$ Nm the coefficient of friction decreases by 3 %. In this comparison the test points with gear geometry Geom A with an oil inlet temperature of $\theta_{oil} = 100$ °C are taken into account. The last comparison shows the influence of the oil temperature on the coefficient of friction. The lowest tested temperature of $\theta_{oil} = 80$°C and the highest temperature of $\theta_{oil} = 120$°C are compared. By increasing the inlet temperature about $\Delta\theta_{oil} = 40$°C the coefficient of friction rises by about 1 %. Both tests were carried out with gear geometry Geom A at a load level of $T_2 = 1900$ Nm.

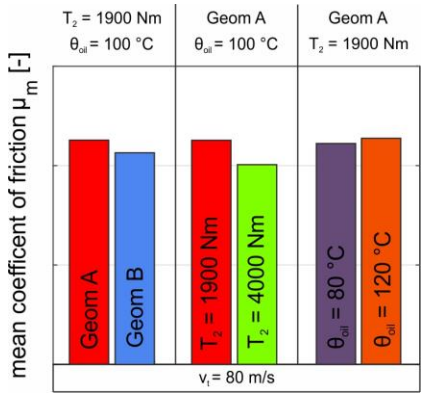

Fig. 7. Influences of gear geometry, load torque and oil temperature on the mean CoF in test results

The results presented in the previous sections show the major influences on the coefficient of friction. By increasing the pitch line velocity, the CoF decreases significantly. Furthermore, the change in the flank topography with the decreased surface roughness lowers the friction coefficient by a significant amount. The influences of the used gear geometry, the applied torque and the oil inlet temperature are significantly lower than the speed influence.

V. FRICTON MODEL

The aim of this work is to develop a model, which can describe the coefficient of friction locally in the gear mesh. The parameter field of the tests carried out is not wide enough to develop a fundamentally new friction model. The previous analyses made clear that the influence of the local velocities is decisive for the evaluation of the coefficient of friction. Because of this fact an existing model, which considers the local slide-to-roll ratio, is used and modified based on the test results. For this approach the friction model developed from LÖPENHAUS [15] is used. It represents an adaptation of the analysis of stationary disk contact in a disc tribometer to spur gear meshing. This model's underlying analyses focus on the tribological properties, particularly the influence of viscosity, elastohydrodynamic speed, load, and radii of curvature. These analyses aim to capture the fundamental relationships between these variables. By mapping these parameters, the model can predict the local coefficient friction during gear meshing. The tested parameter range meets the essential requirements for accurately modeling friction and is particularly useful for determining local friction coefficients in the loaded areas of gear teeth, providing a robust solution for gear tribology studies. Despite this, the calculation approach is not yet calibrated for the test conditions with high pitch line velocities and superfinished gear flanks, used in this work. Therefore, in addition to the linear factor c_1 and the topography factor X_{OS}, the individual influence on the entrainment velocity c_2 was also varied to solve the optimization task. The topography factor differentiates between ground and superfinished flanks. Equation (9) shows the modified model approach.

$$\mu = c_1 \cdot (v_\Sigma)^{c_2} \cdot \exp(c_3 \cdot p) \cdot (c_4 \cdot \eta_M^2 + c_5 \cdot \eta_M + c_6) \cdot Ra^{c_7} \cdot \frac{|S|}{(|S|+c_8)^2+c_9} \cdot \rho_n^{0.2} \cdot X_L \cdot X_{OS} \tag{9}$$

The final parameter set was ultimately the result of multiparametric optimization, which achieved the best possible match between the experimental $P_{V\,ZP,exp}$ and the simulated $P_{V\,ZP,sim}$ data points. The quality of the derived parameters can be described by the coefficient of determination R^2. Fig. 8 shows the comparison of the simulative mean CoF and the evaluated CoF based on the measurements with the test points. After the optimization process this amounts to $R^2 = 93.37\,\%$. All the datapoints were inside of the range of the 25% error band. The colourmap underlines the influence of the pitch line velocity on the friction in the gear mesh.

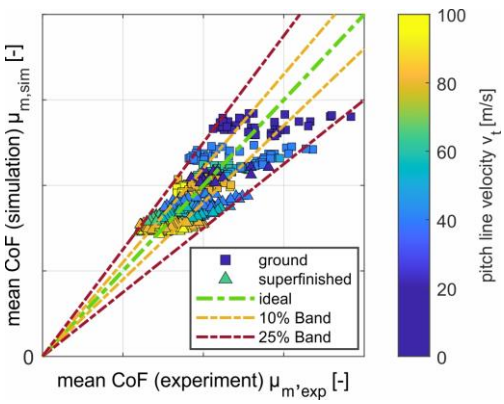

Fig. 8. Comparison of experimental and simulative CoF for all experimental test points

The friction model can be applied on the local loads of the gear mesh from beginning to end of the slide to roll contact. Fig. 9 represents the CoF in gear mesh of the pinion for Geom B with a load of $T_2 = 1900$ Nm for $v_t = 10,\ 50$ and 100 m/s. The CoF has a minimum at the pitch point, where there is just rolling and no sliding of the gear flanks.

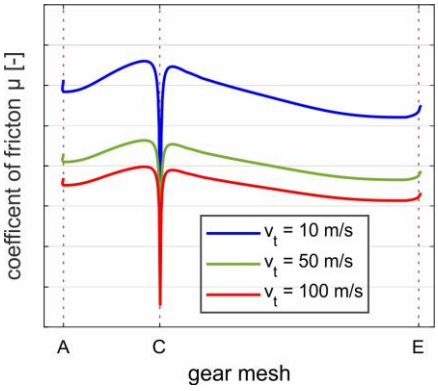

Fig. 9. Local CoF in the gear mesh of a Geom B pinion with $T_2 = 1900$ Nm for pitchline velocites of $v_t = 10, 50$ and 100 m/s

VI. CONCLUSION

This paper presents a calculation approach for the local evaluation of the coefficient of friction in the gear mesh. For the calibration experimental tests on a high-speed back-to-back test rig were carried out. To evaluate the coefficient of friction, the power losses were calculated from the heat dissipation for the gear friction into the lubricant. The difference between the inlet to the outlet temperature is used to conclude the total gear power losses. Based on the test points from varying speed and load levels the experimental mean coefficient of friction is calculated. For the friction model approach an existing model from LÖPENHAUS [15] is used as basis. The coefficients of the model were modified using multiparametric optimization. The calculation method allows to evaluate the coefficient of friction locally in every contact situation of the gear mesh.

The results of the power loss test showed a major speed influence on the coefficient of friction. By increasing the pitch line velocity, the CoF decreases degressively. The variations of

the load torque and the oil inlet temperature were significantly lower within the variation ranges. By applying isotropic superfinishing on the ground gear flanks, the coefficient of friction was reduced by about $\Delta\mu_m = 30$ % over the whole test speed range. The process of superfinishing is a good choice to reduce the coefficient of friction and the resulting gear power losses. This is especially relevant in civil aviation and drive trains in electric powered vehicles.

ACKNOWLEDGMENT

This work was carried out jointly with Rolls-Royce Germany as part of the KOVOHLG research project (funding code: 20T1912). The authors would like to thank Rolls-Royce Germany for their support and for the opportunity to publish this work. The authors would also like to thank the Federal Ministry of Economic Affairs and Climate Action (BMWK) for providing the financial resources.

Symbol	*Denomination*	*unit*
β	Helix angle	°
p	Hertzian Pressure	N/mm²
S	Specific sliding	-
Ra	Arithmetic surface roughness	µm
ρ_{oil}	Densitiy	kg/m³
ρ_n	Radius of curvature	mm
θ_{out}	Outlet temperature	°C
θ_{in}	Inlet temperature	°C
η_M	Kinematik viscositiy at bulk temperature	cSt
ε_α	Overlap	-
δ_z	Contact line deviation	µm
α_n	Normale pressure angle	°
$z_{1,2}$	Number of teeth	-
$x_{1,2}$	Profile shift	-
v_{tb}	Nominal speed at base circle	m/s
v_t	Pitch line velocity	m/s
$v_{t1,2}$	Tangential velocities	m/s
v_g	Sliding velocities	m/s
v_Σ	Entraining speed	m/s
t_E	Engagement time	s
$r_{k,j}$	Radius of contact point	mm
m_n	Normale modulus	mm
l_{eff}	Effective tooth width	mm
f_N	Normal contact force	N
$d_{a1,2}$	Active tip circle	mm
c_p	Heat capacity	kJ/(kg K)
$b_{1,2}$	Active tooth width	mm
a_k	displacement influence number	1/
X_{OS}	Topography factor	-
X_L	Lubricant factor	-
T_1	Pinion Torque	Nm
P_a	Power in tension circle	kW
H_{vL}	Gear geometry power loss factor	-
F_{tb}	Nominal contact force at base circle	N
P_{VZP}	Load dependend power losses	kW
P_{VZ0}	Load independend power losses	kW
P_{VZ}	Gear power losses	kW
μ_m	Mean coefficent of friction	-
$\dot{V}_{oil}$	Oil volume flow	l/min
$\dot{Q}_{oil}$	Heat flow in oil	J/s

REFERENCES

[1] R. W. Snidle and H. P. Evans, "Understanding Scuffing and Micropitting of Gears," Proceedings of the NATO Research and Technology Organization (RTO-MP), pp. 1–18, 2004.

[2] S. Sjöberg, M. Sosa, M. Andersson, and U. Olofsson, "Analysis of efficiency of spur ground gears and the influence of running-in," Tribology International, no. 93, pp. 172–181, 2016, doi: 10.1016/j.triboint.2015.08.045.

[3] J. Vorgerd, P. Tenberge, N. Aufderstroth, and A. Thomas, "Kalorimetrische Messung der Verzahnungsverlustleistung im Bereich hoher Umfangsgeschwindigkeiten," Tribologie und Schmierungstechnik 70, 22 - 30, 2023.

[4] M. Sosa, "Running-in of gears - surface and efficiency transformation," PhD Thesis, KTH, Stockholm, 2017.

[5] H. Linke, Stirnradverzahnung: Berechnung - Werkstoffe - Fertigung. Munich: Hanser, 2010.

[6] J. Vorgerd, P. Tenberge, and M. Joop, "Scuffing of cylindrical gears with pitch line velocities up to 100 m/s," Forschung im Ingenieurwesen, no. 86, pp. 513–520, 2021.

[7] H. Ohlendorf, "Verlustleistung und Erwärmung von Stirnrädern," PhD Thesis, TU Munich, Munich, 1958.

[8] J. A. Wimmer, "Lastverluste von Stirnradverzahnungen: Konstruktive Einflüsse, Wirkungsgradmaximierung, Tribologie," PhD Thesis, TU Munich, Munich, 2006.

[9] W. Mauz, "Hydraulische Verluste von Stirnradgetrieben Bei Umfangsgeschwindigkeiten Bis 60 m/s," PhD Thesis, University Stuttgart, Stuttgart, 1988.

[10] J. Greiner, "Untersuchungen zur Schmierung und Kühlung einspritzgeschmierter Stirnradgetriebe," PhD Thesis, University Stuttgart, Stuttgart, 1990.

[11] L. Schlenk, "Untersuchungen zur Fresstragfähigkeit von Großzahnrädern," PhD Thesis, TU Munich, Munich, 1995.

[12] K. Michaelis, "Die Integraltemperatur zur Beurteilung der Fresstragfähigkeit von Stirnradgetrieben," PhD Thesis, TU Munich, Munich, 1987.

[13] Calculation of load capacity of spur and helical gears - Part 20: Calculation of scuffing load - Flash temperature method, ISO/TS 6336-20, ISO, 2017.

[14] M. Joop, "Die Fresstragfähigkeit von Stirnrädern bei hohen Umfangsgeschwindigkeiten bis 100 m/s," PhD Thesis, Ruhr-University, Bochum, 2018.

[15] C. Löpenhaus, "Untersuchung und Berechnung der Wälzfestigkeit im Scheiben- und Zahnflankenkontakt," PhD Thesis, RWTH Aachen, Aachen, 2015.

[16] G. H. Benedict and B. W. Kelley, "Instantaneous Coefficients of Gear Tooth Friction," ASLE Trans. 4, pp. 59–70, 1961, doi: 10.1080/05698196108972420.

[17] M. Klein, Zur Fresstragfähigkeit von Kegelrad- und Hypoidgetrieben. Dissertation TU München. München, 2012.

[18] F. Prexler, "Einfluss der Wälzflächenrauheit auf die Grübchenbildung vergüteter Scheiben im EHD-Kontakt," PhD Thesis, TU Munich, Munich, 1990.

[19] J. Mayer, "Einfluss der Oberfläche und des Schmierstoffs auf das Reibungsverhalten im EHD-Kontakt," PhD Thesis, TU Munich, Munich, 2013.

[20] F. Klocke and D. Brecher, Zahnrad- und Getriebetechnik: Auslegung - Herstellung - Untersuchung - Simulation, 1st ed.: Carl Hanser, 2017.

[21] H. Prüller, Praxiswissen Gleitschleifen: Leitfaden für die Produktionsplanung und Prozessoptimierung, 2nd ed. Wiesbaden: Springer Vieweg, 2015.

[22] B. D. Hansen, "Scuffing Resistance of Isotropic Superfinished Precision Gears," Gear Solutions 6, 2008.

[23] J. König, "Steigerung der Zahnflankentragfähigkeit durch optimierte Fertigung und Schmierung," PhD Thesis, TU Munich, Munich, 2020.

[24] F. Joachim and N. Kurz, "Influence of surface condition and lubricant on tooth flank capacity," 2016.
[25] Niskanen P.W and Hansen B, Scuffing Resistance of Isotropic Superfinished Precision Gears. AGMA Technical Paper 05FTM13, 2005.
[26] M. Walkowiak, "Örtliche Belastungen und Verschleißsimulation in den Zahneingriffen profilkorrigierter gerad- und schrägverzahnter Stirnräder zwischen Einfederungsbeginn und Ausfederungsende," PhD Thesis, Ruhr-University, Bochum, 2013.